Electrochimica Acta 571 (2026) 148957

Contents lists available at ScienceDirect

Electrochimica Acta

journal homepage: www.journals.elsevier.com/electrochimica-acta

# Extension of electrochemical techniques coupled to non-aqueous capillary electrophoresis towards reduction at silver electrodes

Martin Koall, Frank-Michael Matysik *

*Institute of Analytical Chemistry, Chemo- and Biosensors, University of Regensburg, Universitätsstraße 31, 93053 Regensburg, Germany*

ARTICLE INFO

*Keywords:*
Capillary electrophoresis
Electrochemical detection
Electrochemical reduction
Mass spectrometry
Non-aqueous media

ABSTRACT

While amperometric detection (AD) has been a powerful technique in non-aqueous capillary electrophoresis (NACE) for many years, it has been used only for several oxidative determinations. Since reductive electrochemistry offers many possibilities, this study aims to extend NACE-AD to reductive electrochemical approaches. After electrode material characterization in electrolytes based on acetonitrile (ACN), silver (Ag) emerged as the most suitable electrode material among gold (Au) and platinum (Pt) due to its higher overpotential for hydrogen evolution, and therefore, offers a broader potential range for reductive determinations in conjunction with electrolytes containing ammonium acetate and acetic acid. The applicability of reductive NACE-AD at Ag electrodes was subsequently evaluated using nitrophenolic compounds as model analytes, namely 4-nitrophenol (4NP), 2,4-dinitrophenol (DNP), and 2,4,6-trinitrophenol (TNP). This method enabled the selective detection of each nitrophenol within the migration window for negatively charged species without oxygen removal. It was found that reductive detection in ACN-based NACE was straightforward in the presence of dissolved oxygen, reaching low limits of detection in the μM range (0.5 μM for TNP and 2.0 μM for DNP). Furthermore, mechanistic insight into the electrode reactions was obtained using a newly developed, user-friendly electrochemical injection module for capillary electrophoresis coupled to mass spectrometry (EC—CE-MS), to gain a holistic view of NACE-AD and the electrochemical processes involved. Here, 4-aminophenol, 4-amino-2-nitrophenol, and 4-amino-2,4-dinitrophenol could be identified as the electrode reaction products at a detection potential of - 1.3 V for NACE-AD in ACN-based media.

## 1. Introduction

Capillary electrophoresis (CE) is a highly efficient separation technique that requires minimal sample and solvent volumes, making it suitable for a wide range of analytical applications. Non-aqueous capillary electrophoresis (NACE) enhances CE by enabling the separation of compounds poorly compatible with aqueous media while also providing better long-term stability and lower electrophoretic currents [1] compared to its aqueous counterpart. NACE is especially valuable in pharmaceutical, environmental, and analytical contexts for handling poorly water-soluble substances [2]. Commonly, NACE is combined with conductivity [3–5], mass spectrometric [5–7], and UV [8,9] detection. A less common, but powerful detection principle in NACE is amperometric detection (AD), relying on the electrochemical activity of various analytes. In this context, NACE-AD shows improved sensitivity, selectivity, and stability, aided by the use of organic solvents that reduce noise and enhance detection performance [10]. NACE-AD has been utilized to determine chlorinated phenols [11], illicit drugs [12,13], nicotine in tobacco [14], and nicarbazine (coccidiostat) in poultry feed [15]. Furthermore, a novel dual-detection concept based on NACE-AD and mass spectrometry has been successfully deployed for the sensitive and selective determination of trimetazidine (doping agent) in urine [16] and nitenpyram (pesticide) in pet medication [17]. However, all the above-mentioned methods rely on NACE in combination with oxidative AD.

Notably, no method has yet been reported that uses a reductive NACE-AD approach, although reduction plays an important role in many electrochemical fields. For example, reductive electrochemical detection in aqueous CE has enabled the analysis of various analytes, such as inorganic peroxides with gold (Au) microelectrodes [18], explosives with Au and Ag electrodes [19], and nitrophenols with carbon fiber electrodes [20]. Entirely non-aqueous systems have also been used for reductive processes, for example, the electrosynthesis of fluorinated compounds from dichlorofluoromethane [21], voltammetric reduction

* Corresponding author.
*E-mail address:* frank-michael.matysik@chemie.uni-r.de (F.-M. Matysik).

https://doi.org/10.1016/j.electacta.2026.148957
Received 12 March 2026; Received in revised form 14 April 2026; Accepted 26 April 2026
Available online 30 April 2026

of benzamide [22], and detection of patulin and 5-hydroxymethylfurfural in apple juice [23]. Given this background, the integration of NACE with reductive AD in non-aqueous background electrolytes (BGEs) could be a promising new option in various analyses. For example, a typical NACE BGE based on acetic acid and ammonium acetate dissolved in ACN, which has been utilized in several oxidative NACE-AD applications [14–17], could also be beneficial in this context since acetic acid can provide protons needed in electrochemical reductions.

Nitrophenols present an important class of reducible compounds. They are widely used in the production of pesticides, dyes, explosives, and pharmaceuticals, but are latent, toxic, and environmentally hazardous if not properly controlled. Typically, elevated concentration levels of nitrophenols have been found in water and soil samples near industry due to insufficiently treated wastewater [24] and military training grounds and facilities [25] due to the production and use of ammunition containing 2,4-dinitrophenol (DNP) and 2,4,6-trinitrophenol (TNP) as explosives. Structurally, NPs have one or more nitro groups attached to a phenol ring, at the ortho, meta, or para position. These nitro groups can be targeted by electrochemical reduction. The respective hydroxylamino- and amino species have been reported as the main electrode reaction products for the electrochemical reduction of various nitrocompounds, including nitrophenols, in aqueous media [26–31]. Additionally, nitrophenols exhibit a negative charge in media containing acetonitrile (ACN) due to the combined effects of deprotonation and hyperconjugation, and can therefore be easily separated by NACE [32,33].

Given this perspective, we present the introduction to reductive AD in the field of NACE. As a starting point, possible electrode materials (Au, Ag, and Pt) were characterized in ACN BGE by cyclic voltammetry (CV), with Ag emerging as the most promising candidate. 4-nitrophenol (4NP), DNP, and TNP were used as model analytes, investigating the electrochemical characteristics, migration behavior, and analytical performance of reductive NACE-AD regarding nitrophenols. In this approach, the oxygen reduction reaction (ORR) appeared as a constant background signal, and thus, reductive detection in ACN-based NACE was straightforward in the presence of dissolved oxygen. Moreover, the products of the electrode reactions during detection were investigated via electrochemically assisted injection to CE coupled to mass spectrometry (EC—CE-MS), which has been previously described for oxidative NACE-AD determination, utilizing special injection modules [15, 17]. This project aims to extend the application of NACE-AD, non-aqueous EC—CE-MS, and dual-detection concepts based on NACE-AD and to give opportunities for efficient nitrophenol monitoring.

## 2. Experimental

### 2.1. Materials and reagents

The following chemicals were used, all of analytical grade: 2,4-dinitrophenol (DNP), 2,4,6-trinitrophenol (TNP), 4-amino-2-nitrophenol, and 4-aminophenol (4AP) were purchased from Sigma-Aldrich (St. Louis, USA). 4-nitrophenol (4NP) and hydrazine hydrate were supplied by Fluka Chemie GmbH (Buchs, Switzerland). Acetonitrile (ACN), ammonium acetate, 0.1 M sodium hydroxide solution, and formic acid were purchased from Merck (Darmstadt, Germany). Acetic acid and 2-propanol were purchased from Carl Roth (Karlsruhe, Germany). Ultrapure water was provided by a Milli-Q Advantage A10 system (Merck Darmstadt, Germany). All measurements were carried out using a background electrolyte consisting of 1 M acetic acid and 10 mM ammonium acetate in ACN.

Fused silica capillaries (75 μm inner diameter, 365 μm outer diameter, polyimide coated) were purchased from Polymicro Technologies (Phoenix, USA). For the preparation of the AD electrodes, 25 μm Ag, Pt wires provided by Advent Research Materials (Oxford, United Kingdom) and 25 μm Au wires supplied by Goodfellow (Cambridge, United Kingdom) were used.

### 2.2. Experimental procedures

#### 2.2.1. Micro-electrode fabrication

The micro-electrodes were manufactured after the following procedure: Firstly, the soda glass capillary (O.D. 350 μm, wall thickness 103 μm, length: 100 mm) from Hilgenberg GmbH (Malsfeld, Germany) was cut into 20 mm-long pieces. After closing one capillary end using heat treatment, the wire was inserted. Finally, the wire was completely sealed in the glass capillary by applying heat and a vacuum. This procedure was chosen to achieve the best possible sealing while applying minimal heat, since the Ag and Au micro-wires were prone to melting due to their lower melting points compared to Pt. The sealed electrodes were embedded in laboratory-crafted PTFE fittings and glued to copper tubing using silver epoxy from M.G. Chemicals (Burlington, Canada) for electrical connection.

The same strategy was applied to all electrodes, which were deployed in the CV experiments.

#### 2.2.2. Synthesis of 4-amino-2,6-dinitrophenol

4-amino-2,6-dinitrophenol was synthesized as an analytical standard using Cu nanoparticles as a catalyst and 2,4,6-trinitrophenol* as a starting material. Firstly, Cu nanoparticles were synthesized by reducing an aqueous $CuSO_4$ solution (50 mL, 10 mM) by adding 20 mM hydrazine hydrate under stirring at room temperature. Afterward, the mixture was heated to 60 °C for 30 min. TNP (4.4 mM) and hydrazine hydrate (10 mM) were dissolved in 50 mL ACN and added to the aqueous medium. The mixture was kept at 60 °C for one additional hour. The initially yellow solution changed color to red. As a next step, the solution was filtered to remove the nanoparticles. Finally, the solvent was removed, and the red precipitate was collected.

The crude product was purified by recrystallization from ACN/$H_2O$ 3/1 (v/v), and characterized by CE-MS.

*2,4,6-trinitrophenol is a potentially explosive compound whose hazard is strongly dependent on its hydration state. The dry material is highly sensitive to shock, friction, and heat, and must therefore be strictly maintained in a wetted condition at all times.

#### 2.2.3. Cyclic voltammetry

The electrochemical behavior of Ag, Au, and Pt electrodes was characterized using CV measurements. For the investigation, a three-electrode setup in a 3-mL batch cell was used. The electrode system was based on an Ag/AgCl reference electrode, a stainless-steel cannula used as a counter electrode, and a 25 μm disc electrode made from the respective metal. The setup was connected to a SP 200 potentiostat from Biologic (Seyssinet-Pariset, France) operated using EC-Lab V11.46 software.

#### 2.2.4. Capillary electrophoresis with amperometric detection

A custom-built, LabVIEW-controlled CE-system [17] was coupled to an in-house constructed AD cell, which is described in [10] in detail. This cell configuration was utilized in all CE-AD experiments. A schematic representation of the CE-AD setup can be found in **Fig. S5**.

Briefly, the AD cell featured a three-electrode system. A 25 μm Ag disk electrode served as the working electrode, while an Ag/AgCl wire acted as the reference electrode. A stainless-steel tube, which also functioned as the capillary guide, served as the auxiliary electrode and was grounded to complete the CE circuit. Electrode alignment was performed under an UltraZoom Pro digital microscope (dnt, Dietzenbach, Germany). The AD cell was enclosed in a custom-built Faraday cage to minimize electromagnetic interference. The three-electrode assembly was connected to a BioLogic SP-200 potentiostat equipped with an ultralow current module (BioLogic, Seyssinet-Pariset, France) and operated using EC-Lab V11.46 software. The sample was injected for 10 s by a syphon effect due to a difference in height between the capillary inlet and outlet of 15 cm.

The separation capillary (length, 65 cm; I.D., 75 μm) was prepared

according to the following procedure: the capillary ends were polished at a 90° angle and sequentially rinsed with 0.1 M NaOH (10 min), deionized water (5 min), and background electrolyte (BGE: 10 mM ammonium acetate and 1 M acetic acid in ACN, 30 min). The capillary was subsequently stored overnight in ACN.

### 2.2.5. Mechanistic investigations

For the investigation of the electrode processes, an advanced electrochemical injection module evolved from our previous work [17] was used. This injection cell was developed to utilize a cylindrical standard electrode commonly used as a working electrode (WE) in electrochemical measurements. Moreover, the design was modified to accommodate a removable auxiliary and reference electrode to enable easy replacement of all electrodes in the case of the characterization of different materials or electrode fouling. A 3D model of the module can be seen in Fig. 1(1), and explosion drawings of relevant cell details are shown in Fig. 1(2–4).

The cell was based on a PTFE body and a stainless-steel cell cover. The cap held a sample reservoir made from a modified micro-insert (0.3 ml) from Avantor (Radnor, USA). Auxiliary electrode (stainless-steel cannula) and reference electrode (Ag/AgCl wire) were integrated into the reservoir. The separation capillary was guided through a glass funnel made from a modified disposable Pasteur pipette from Avantor (Radnor, USA). The working electrode (WE, **see** Fig. 1(4)) consisted of a 3 mm disc housed in a PTFE body and was held in place by a copper screw, which also served as a connector to the potentiostat. In this work, Ag was used as the WE material. A detailed view of the electrode system can be seen in Fig. 1(3). The cell was sealed with a modified silicone septum E158.1 from Carl Roth (Karlsruhe, Germany) as a gasket. The arrangement was compressed by four threaded rods and eight hexagonal nuts (M2). The injection module was connected to a μAutolab potentiostat/galvanostat (Metrohm Autolab B. V., Utrecht, Netherlands) to apply the WE potential. The injection cell could be placed in the autosampler of the CE device, analogous to a standard vial (1.5 ml, ND 9) from Avantor (Radnor, USA). For the injection of the sample from the electrode surface, the position of the high-voltage electrode and capillary was optimized with the help of the capillary positioning system of the laboratory-constructed CE device [17]. The unique cell design allows the use of a multitude of common electrode materials like boron-doped diamond, glassy carbon, metals (e. g., Ag, Au, Pt, and many more) as WEs. Furthermore, sample reservoir, auxiliary, reference, and working electrodes could also be replaced easily, which is especially desirable when working under corrosive conditions.

The electrode reaction was investigated by EC—CE-MS in combination with the newly developed injection module. A schematic representation of the EC—CE-MS setup, utilizing specialized injection modules, can be seen in **Fig. S6**. 4NP, DNP, and TNP (500 μM in BGE), and blank BGE were injected from the surface of the WE while a potential of - 1.3 V vs. Ag/AgCl was applied. Prior to injection, the electrochemical injection module was kept at - 1.3 V for 60 s to provide a steady-state concentration of the analytes with subsequent CE separation at 8 kV. 4NP, DNP, TNP, and 4-aminophenol (4AP), 4-amino-2-nitrophenol (ANP), and 4-amino-2,6-dinitrophenol (ADNP), which were the suspected reduction products of the respective nitrophenol, were also injected at open circuit potential (OCP). All solutions contained 500 μM of the respective analyte in BGE. A micrOTOF mass spectrometer from Bruker Daltonics (Bremen, Germany) with a coaxial sheath-flow ESI interface from Agilent Technologies (Santa Clara, USA) was used for mass spectrometry. For the detection of DNP, TNP, and the respective products of electrochemical reduction, the micrOTOF mass spectrometer was operated in negative ion polarity mode using a sheath-liquid consisting of $H_2O$:2-propanol:ammonia (49.975:49.975:0.05, v:v:v). The device was operated with the following parameters: nebulizer gas pressure 0.3 bar, dry gas ($N_2$) flow 2.5 L/min, dry gas temperature 240 °C, and $m/z$ 50–400. The sheath liquid had a flow rate of 480 μl/h. For the detection of 4NP, the micrOTOF mass spectrometer was operated in positive ion polarity mode using a sheath-liquid consisting of $H_2O$:2-propanol:formic acid (49.95:49.95:0.1, v:v:v). The device was operated with the following parameters: nebulizer gas pressure 0.3 bar, dry gas ($N_2$) flow 2.5 L/min, dry gas temperature 240 °C, and $m/z$ 50–400. The sheath liquid had a flow rate of 480 μl/h. Data Analysis 4.0 SP1 from Bruker Daltonics (Bremen, Germany) and MZmine 3 [34] were used for data acquisition.

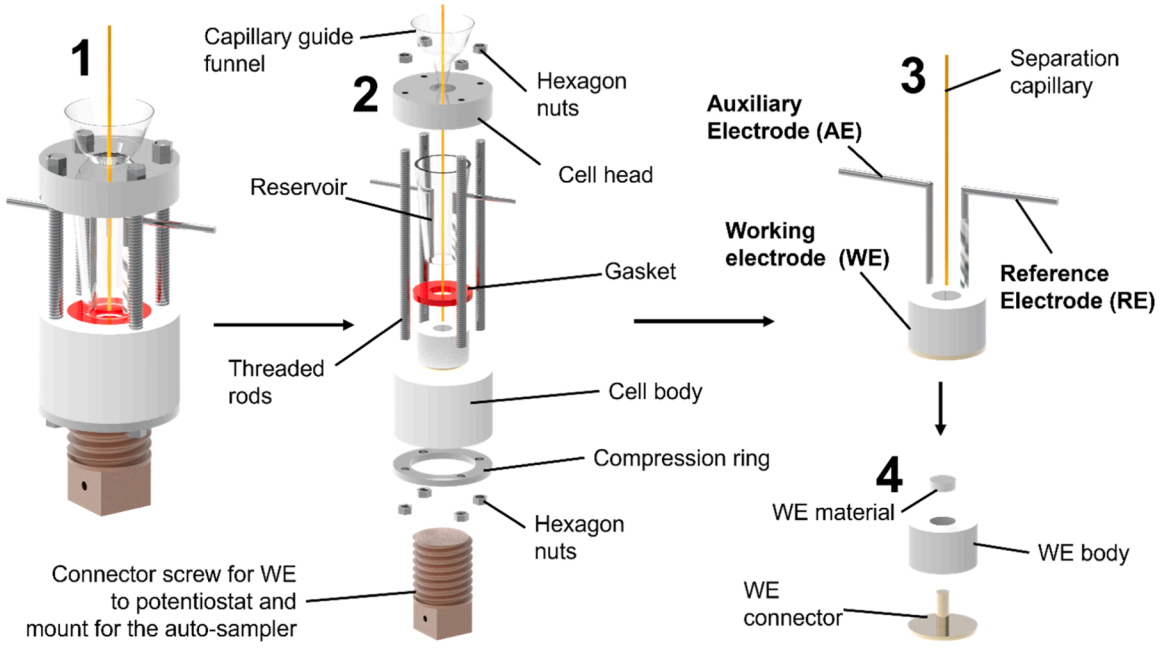


**Fig. 1.** Novel design for an electrochemical injection module for CE. 1: Full 3D model of the cell. 2: Explosion model of the cell. 3: Zoomed-in view of the electrode system. 4: Explosion view of the WE composition.

## 3. Results and discussion

### 3.1. Electrochemical characterization of electrode materials for non-aqueous capillary electrophoresis with amperometric detection

As reductive detection poses a new field in NACE-AD, different electrode materials were tested for their applicability in this context. The noble metals Ag, Au, and Pt were chosen due to their stability in the investigated BGE (10 mM ammonium acetate and 1 M acetic acid in ACN) and the availability of micro wires for the production of ultra-micro electrodes. For the material characterization, CV was performed from 0 to - 1.5 V in BGE in the presence of dissolved oxygen, resulting in the different current responses shown in Fig. 2.

Firstly, the oxygen reduction reaction (ORR) showed similar onset potentials at approximately - 0.4 V for all materials investigated. Different ORR mechanisms have been proposed for the respective metals [35–37]. The second important electrode reaction to consider is the hydrogen evolution reaction (HER). Here, Ag, Au, and Pt differed significantly from each other. For Pt, HER started at - 0.9 V, marking the lower end of the electrochemically stable potential range in combination with the BGE (10 mM ammonium acetate and 1 M acetic acid in ACN). This could be attributed to the high catalytic activity of Pt in the HER. On the contrary, Au showed low activity, and Ag even lower activity, which has also been reflected in the exchange current densities for Ag, Au, and Pt reported by Lasia et al. [38] for HER determined in aqueous media. The same trend for more negative HER potentials for Au (- 1.1 V) and Ag (- 1.3 V) could be observed in this work. This led to a wider range in negative potentials for reductive determinations of the systems Au|ACN BGE and Ag|ACN BGE before HER took over. At this point, Ag emerged as the best-suited electrode material exhibiting the largest potential range for reductive AD. All the following experiments were carried out using 25 µm Ag micro-disc electrodes.

The next point to be addressed was the electrochemical behavior of the electrode during CE separation. For oxidative NACE-AD, a potential shift has been reported when positive HV is applied in end-capillary AD, which had to be accounted for by adding an extra-potential [14]. A similar situation could be encountered using reductive NACE-AD. To compensate, the potential shift (ΔE) was subtracted from the optimum detection potential of each analyte when no separation voltage was applied, to achieve low background currents and sensitive AD with a positive separation voltage (see supporting information **Fig. S. 1**).

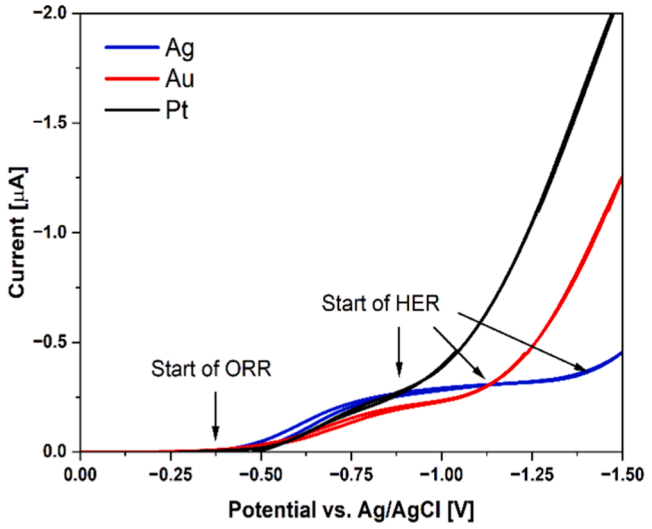


**Fig. 2.** Comparison of CV measurements of different electrode materials in BGE (10 mM ammonium acetate and 1 M acetic acid in ACN) in the presence of dissolved oxygen. Cyclic voltammograms of 25 µm disc electrodes made of silver (Ag, blue), gold (Au, red), and platinum (Pt, black). Start of oxygen reduction reaction (ORR) and hydrogen evolution reaction (HER) at different potentials for Ag, Au, and Pt. Scan rate: 50 mV/s.

### 3.2. Investigation of nitrophenolic compounds

#### 3.2.1. Electrochemical properties of nitrophenols in ACN BGE

In the context of electrochemical detection methods, the choice of electrode material is crucial, as the electrode forms the interface between the analyte and the electronic measurement system. Therefore, different electrode materials can significantly influence sensitivity, selectivity, and stability. For a first proof-of-concept, differently substituted nitrophenolic compounds, namely TNP, DNP, and 4NP, were chosen as model substances.

All compounds contain one or more nitro groups, which can be electrochemically reduced. The species differ in the number and position of the nitro groups to investigate the influence of substituents on electrochemistry, electrochemical products, and CE separation. As a first step in the electrochemical characterization, cyclic voltammograms of 1 mM solutions of TNP, DNP, and 4NP were performed using Ag and Pt micro-disc electrodes and compared with BGE. The corresponding CV measurements can be seen in Fig. 3. Here, the same ORR and HER as previously shown in Fig. 2 could be observed in BGE for both electrodes. However, an increased reduction current could be found for all solutions of TNP, DNP, and 4NP at the Ag electrode (starting at – 0.8 V), indicating additional electrochemical reduction. Signal intensity and onset do not differ significantly, suggesting similar reduction mechanisms for all compounds investigated. Moreover, a comparison with Pt under the same conditions showed a lack of change in reduction current. This led to the conclusion that Ag showed electrocatalytic activity for the reduction of nitrophenols and was therefore ideally suited for the detection of TNP, DNP, and 4NP in the context of reductive NACE-AD. It is important to note that although ORR potential and the reduction of nitrophenols may overlap, CV provided a clear difference in signal for BGE and the analyte solution, which could be translated to AD. Removing oxygen could be challenging due to the fast diffusion and high solubility of $O_2$ [39] in ACN compared to other media and the high volatility of ACN and acetic acid. This is particularly relevant for reliable NACE operation. For this reason, it was decided to continue all further experiments without removing oxygen.

#### 3.2.2. Analytical characterization of nitrophenols in ACN BGE

Given the electrochemical detectability of nitrophenols in ACN BGE using electrochemical reduction at Ag electrodes, the next step was to obtain the first actual electropherograms of reductive NACE-AD. Here, the migration behavior of TNP, DNP, and 4NP in ACN BGE was investigated. The electropherogram of a mixture of 100 µM TNP, DNP, and 4NP is shown in Fig. 4**, left panel**. 2,4-dinitrotoluene (100 µM, DNT) was added as an EOF-marker. This measurement was performed with low separation voltage (8 kV) to provide an overview of all three nitrophenolic compounds. The electropherogram shows three distinct signals. The comparison with DNT led to the conclusion that all nitrophenols could be detected within the migration window for negatively charged substances (hence showing deprotonation) in the BGE investigated. Furthermore, the degree of negative charge is significantly influenced by the degree of $NO_2$-substitution. While 4NP ($1xNO_2$) migrated close to the EOF, DNP ($2xNO_2$) showed good separation (peak at 575 s), and TNP ($3xNO_2$) could be determined selectively due to its long migration time of 915 s at a separation voltage of 8 kV. This configuration could be used to determine TNP and DNP selectively amongst other nitro compounds. However, 4NP also showed a comparably low negative charge (migration slightly after DNT, visible as a signal shoulder). 4NP could also be determined selectively by enhancing separation efficiency (see Fig. 4, **right panel**). Here, a separation voltage of 27 kV was used to separate a mixture of 500 µM DNT and 4NP, which could not be baseline separated at 8 kV (see Fig. 4, **left panel**). Here, the two species could be separated, and 4NP could be determined

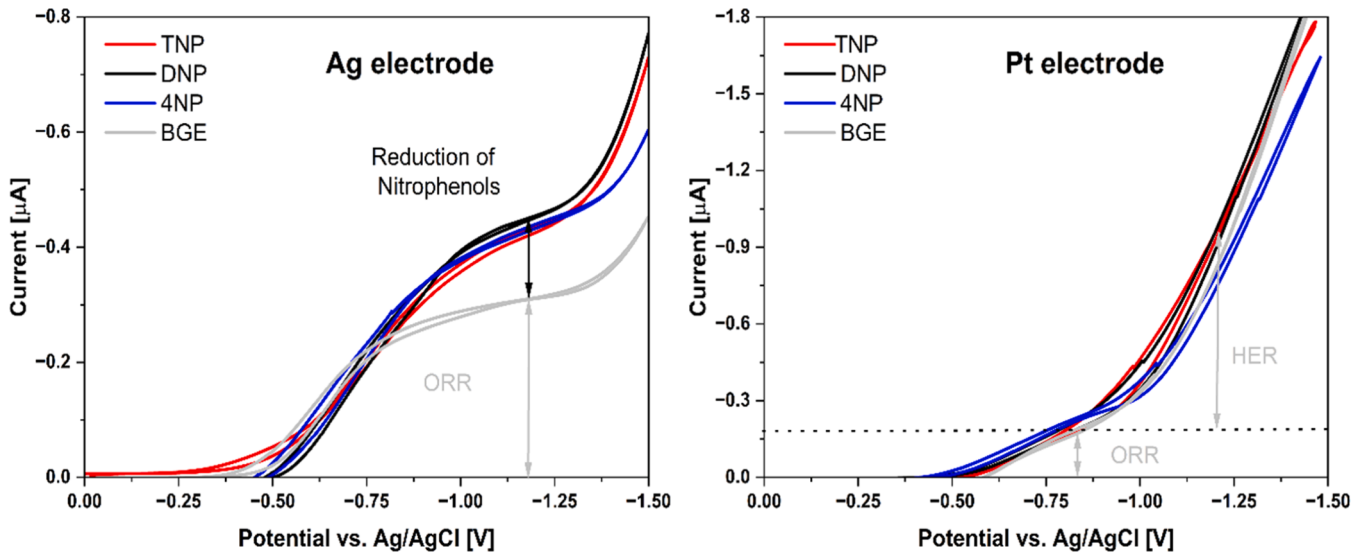


**Fig. 3.** Cyclic voltammograms of differently substituted nitrophenols at Ag and Pt electrodes: 1 mM 2,4,6-trinitrophenol (TNP, red); 2,4-dinitrophenol (DNP, black); 4-nitrophenol (4NP, blue) solutions in BGE (10 mM ammonium acetate and 1 M acetic acid in ACN). Comparison with BGE (grey). All measurements were performed in the presence of oxygen. Visualization of the analyte reduction, oxygen reduction reaction (ORR), and Hydrogen evolution reaction (HER). The current response for nitrophenol reduction could be observed only on the Ag electrode. Scan rate: 50 mV/s.

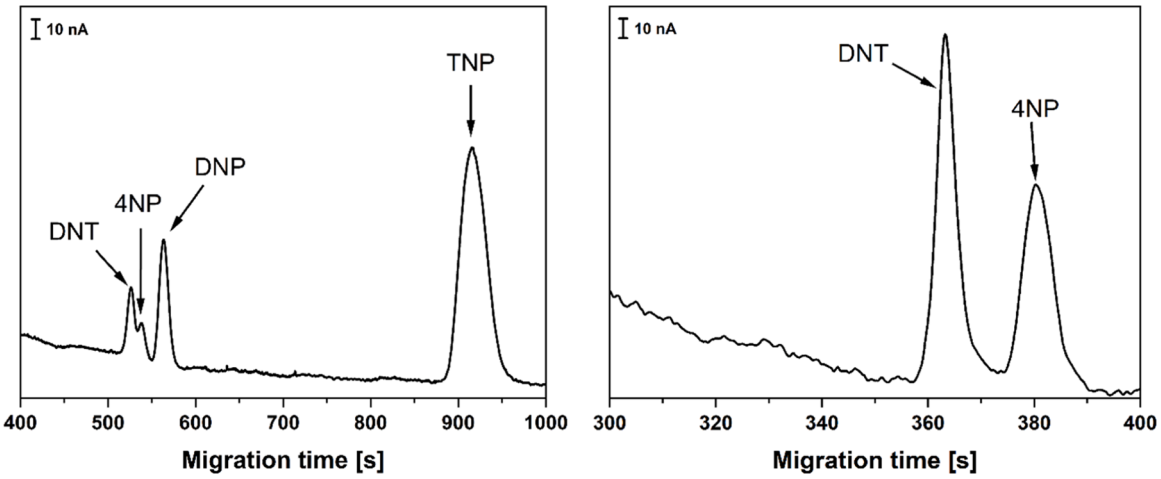


**Fig. 4.** Migration behavior of 4-nitrophenol (4NP), 2,4-dinitrophenol (DNP), and 2,4,6-trinitrophenol (TNP) in BGE (10 mM ammonium acetate and 1 M acetic acid in ACN). 2,4-dinitrotoluene (100 µM, DNT) was used as an EOF marker. Detection at - 1.3 V vs Ag/AgCl using a 25 µm Ag disk electrode. **Left**: Measurements of a 100 µM mixture of 4NP, DNP, TNP, and DNT at a separation voltage of 8 kV. **Right**: Measurements of a 500 µM mixture of 4NP and DNT, at a separation voltage of 27 kV.

selectively. However, due to the much higher separation voltage, the noise level was also increased, which could influence detection performance drastically.

Since only DNP and TNP showed a selective migration behavior at a separation voltage of 8 kV, limits of detection (LODs) were calculated for DNP and TNP, respectively, using a mixture of 4NP, DNP, and TNP in the concentration range from 1 to 5 µM. For 4NP, additional measurements using a mixture of DNT and 4NP in a concentration range from 100 to 500 µM at 27 kV were conducted. The results are summarized in Table 1

**Table 1**
LODs (mean and standard deviation) for the determination of 4NP at a separation voltage of 27 kV, DNP, and TNP at a separation voltage of 8 kV for S/N = 3, (n = 3).

| Analyte | 4NP | DNP | TNP |
|---|---|---|---|
| **Separation voltage [kV]** | 27 | 8 | 8 |
| **LOD [µM]** | $1.0{\cdot}10^{2}\pm 0.1{\cdot}10^{2}$ | 2.0 ± 0.1 | 0.52 ± 0.03 |

for DNP and TNP with LODs in µMrange (0.5 µM for TNP and 2 µM for DNP). A different electrochemical behavior of 4NP under CE-AD conditions (due to the influence of the significantly higher separation voltage) and higher noise levels (see Fig. 4) at 27 kV compared to a separation at 8 kV could contribute to the significantly higher LOD of 4NP (100 µM) compared to DNP and TNP. All LODs were determined for S/N = 3.

### *3.3. Characterization of the electrochemical reduction products for 4-nitrophenol, 2,4-dinitrophenol, and 2,4,6-trinitrophenol*

For the following experiments, the newly developed injection module was equipped with a 3 mm Ag disc electrode as a working electrode (See Fig. 1), and the injection into the CE system was performed from the surface of the working electrode.

#### *3.3.1. Reduction of the BGE*

As a first step in the characterization of the electrode reactions

during AD, the reduction of ACN BGE was investigated. For this purpose, BGE (10 mM ammonium acetate and 1 M acetic acid in ACN) was injected at OCP, and an AD detection potential of - 1.3 V was applied to the injection module while operating the mass spectrometer in negative ion polarity mode. The corresponding total ion electropherograms (TIEs) can be seen in Fig. 5. Here, only the unspecific EOF signal (see black mass spectrum, **right side**) could be observed for injection at OCP, while for injection at - 1.3 V, an additional peak in the migration window for positively charged analytes at 380 s could be observed, hinting a reduction of BGE constituents. The BGE reduction product, characterized by *m/z* 232.8 and *m/z* 134.8 (blue mass spectrum, **left side**), could also be found in the following investigations of 4NP, DNP, and TNP in ACN BGE. For positive ion polarity, no specific electrochemical reduction product could be found for ACN BGE. For the sake of simplicity, the additional illustration of extracted ion electropherograms for this BGE reduction product has been omitted below, since the signal showed a selective migration behavior and could be separated from 4NP, DNP, TNP, and their reduction products by CE.

### 3.3.2. *Reduction of nitrophenolic compounds*

EC—CE-MS was performed to investigate the reduction processes of 4NP, DNP, and TNP at Ag electrodes in ACN BGE. 500 µM 4NP, DNP, and TNP in BGE were investigated. The corresponding electropherograms are shown in Fig. 6. The sample was injected at OCP, and at a potential of - 1.3 V from the surface of the working electrode. For TNP and DNP, mass spectrometric measurements were performed in negative ion polarity mode (see Fig. 6**, top**). For TNP and DNP (black electropherograms), only one signal could be observed, corresponding to the respective $[M\text{-}H]^-$ with *m/z* values of 183.0 for DNP (migration time 615 s) and *m/z* 228.0 for TNP (migration time 975 s), see respective mass spectra in the supporting information (**Fig. S. 2**) when injected at OCP. At - 1.3 V, one additional signal could be observed for each compound for TNP at 580 s and for DNP at 570 s. A comparison with 500 µM solutions of 4-amino-2,6-dinitrophenol (*m/z* 198.0, $[M\text{-}H]^-$) in the case of the reduction of TNP and 4-amino-2-nitrophenol (*m/z* 153.0, $[M\text{-}H]^-$) for DNP (blue electropherograms) suggests an electrochemical conversion of one nitro group to the corresponding amino group. For ADNP, a small residue of TNP could also be found as a contaminant (extracted ion electropherogram *m/z* 228.0) due to the synthesis of ADNP using TNP as a starting material (see Section 2.2.2).

The respective mass spectra are displayed in the supporting information (**Fig. S. 3.1–3**). The EC—CE-MS measurements of 4NP are displayed in Fig. 6, **bottom**. Since no product species were observable in negative ion polarity mode, the investigation of 4NP required the mass spectrometer to be operated in positive ion polarity mode. However, for 4NP, a mass spectrometric response was only observable in negative ion polarity mode. Therefore, an extracted ion electropherogram (*m/z*, 138.1, $[M\text{-}H]^-$, black electropherogram, peak at 575 s) was added to visualize the migration behavior of 4NP. In positive ion polarity mode, no signal could be obtained at OCP, while a signal at 515 s was observed when a potential of - 1.3 V was applied. A comparison with a 500 µM solution of 4-aminophenol (*m/z* 110.0, $[M + H]^+$) injected at OCP suggested the same electrochemical reduction behavior as the other nitrophenolic compounds investigated. The corresponding mass spectra are shown in the supporting information (**Fig. S. 4.1–2**). Furthermore, DNP and TNP exhibited similar electrochemical transitions during the ESI process, as indicated by extracted ion electropherograms showing signals at *m/z* 198.0 and *m/z* 153.0 below the respective $[M\text{–}H]^-$ signals, which were separated from ANP and ADNP by CE.

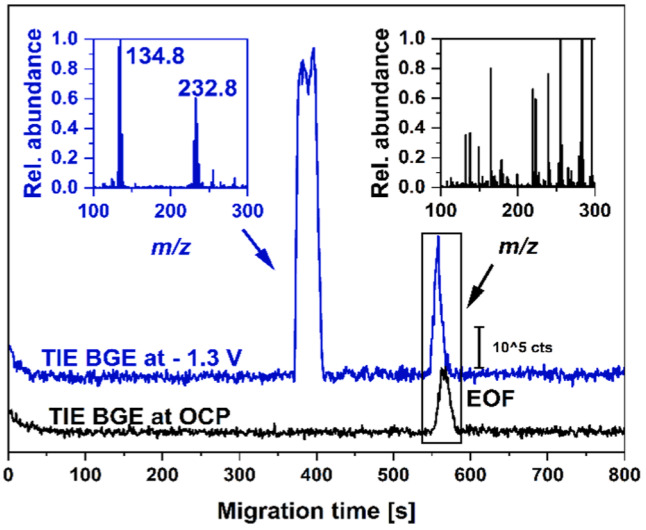


**Fig. 5.** EC—CE-MS measurements of BGE. Total ion electropherograms (TIE) of BGE (10 mM ammonium acetate and 1 M acetic acid in ACN) injected at OCP and - 1.3 V. The CE separation was carried out at 8 kV. Mass spectra obtained from the peaks at 380 s and 575 s.

The EC—CE-MS measurements showed, in agreement with Fig. 3, that all three compounds undergo the same selective transition by the electrochemical reduction of only one nitro group at - 1.3 V in the investigated BGE (10 mM ammonium acetate and 1 M acetic acid in ACN) to the respective amino group. These findings are based on comparisons of migration behavior and mass spectra for the nitrophenol, the electrode reaction products, and the respective amino derivative (used as an analytical standard). However, the ESI ionization behavior of the electrochemical reduction products 4AP, ANP, and ADNP could differ significantly due to the different $-NO_2$ substitution pattern. A schematic summary of the electrode reactions during reductive amperometric detection, and chemical formulas, can be seen in Fig. 7.

In contrast to reports mentioning the reduction of nitrophenols in aqueous media [32], no additional hydroxylamine species could be found for the investigated BGE (10 mM ammonium acetate and 1 M acetic acid in ACN) at a potential of – 1.3 V, suggesting a different electrochemical reduction mechanism in ACN-based BGEs compared to aqueous media.

## 4. Conclusions

In this study, we demonstrated opportunities offered by reductive electrochemical methods in combination with NACE, namely NACE-AD and EC—CE-MS, under NACE conditions. Starting with material characterization in ACN-based media, Ag emerged as the best electrode material for reductive applications due to its high overpotential for HER and stable ORR, resulting in lower background currents than Pt and Au. Furthermore, the possible application of reductive NACE-AD at Ag electrodes was investigated using nitrophenolic compounds as model analytes, resulting in selective migration times within the migration window for negatively charged analytes. AD of the nitrophenols in the presence of dissolved oxygen emerged as a straightforward approach leading to low LODs (0.5 µM for TNP and 2.0 µM for DNP). Given this analytical background, reductive NACE-AD could provide a basis for methods for the sensitive and selective determination of nitrophenols in samples of different origins (surface water, soil, ammunition). Furthermore, insight into the electrode reaction could be gained by the implementation of a newly developed user-friendly electrochemical injection module, which was specifically designed to accommodate a great variety of working electrode materials. The use of 3 mm Ag disc electrodes in combination with ACN BGEs led to the electrochemical reduction of only one nitro group in mono-, di-, and tri-substituted nitrophenols, providing 4AP, ANP, and ADNP selectively at −1.3 V for NACE-AD of the respective nitrophenol. Based on these findings, reductive NACE-AD and EC—CE-MS could be extended to other important substance classes and become an integral part of the CE and electrochemical landscape.

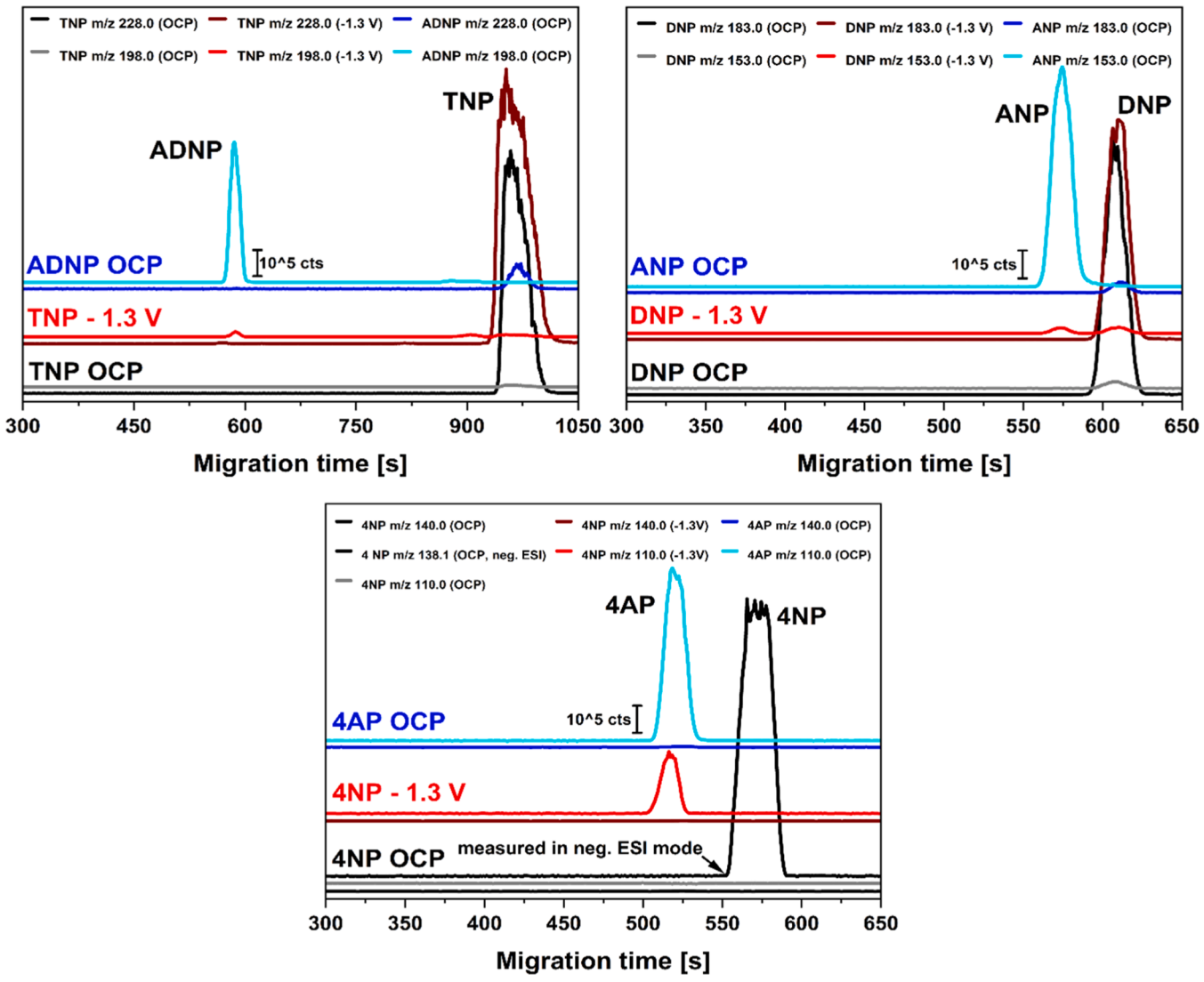


**Fig. 6.** EC—CE-MS measurement of 500 μM solutions of TNP (**top left**), DNP (**top right**), and 4NP (**bottom**) in BGE (10 mM ammonium acetate and 1 M acetic acid in ACN). Extracted ion electropherograms for measurements using *m/z* values of $[M\text{-}H]^-$ for TNP and DNP and their electrochemical reduction products 4-amino-2,6-dinitrophenol (ADNP) and 4-amino-2-nitrophenol (ANP) (negative ion polarity mode), and $[M + H]^+$ for 4NP and the corresponding electrochemical reduction product 4-aminophenol (4AP). The respective mass spectra are shown in the supporting information (**Fig S. 2 – S4**). Injection at open circuit potential (OCP, black electropherograms) and - 1.3 V (red electropherograms) for each nitrophenol. Extracted ion electropherograms of 500 μM solutions of ADNP, ANP, and 4AP injected at OCP (blue electropherograms). An extracted ion electropherogram 4NP $[M\text{-}H]^-$ (measured in negative ion polarity mode, black) was added since no $[M + H]^+$ could be observed for 4NP in positive ion polarity mode. CE conditions are as in Fig. 5.

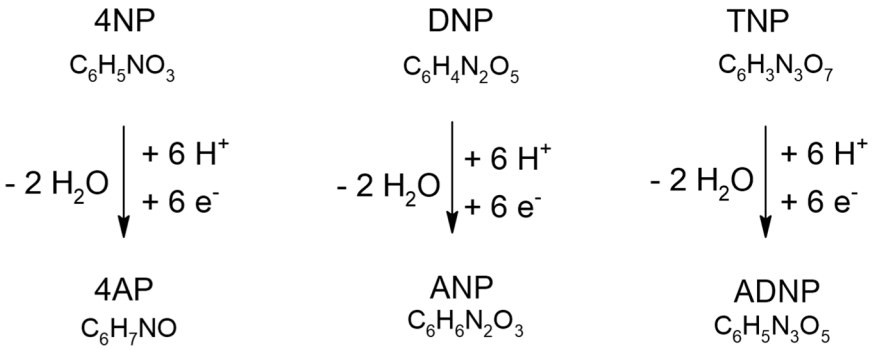


**Fig. 7.** Schematic representation of the electrochemical reduction of 4NP, DNP, and TNP to 4AP, ANP, and ADNP in BGE (10 mM ammonium acetate and 1 M acetic acid in ACN).

## Funding

This work was supported by the Deutsche Forschungsgemeinschaft (DFG) [MA1491/12–3].

## CRediT authorship contribution statement

**Martin Koall:** Writing – original draft, Investigation, Conceptualization. **Frank-Michael Matysik:** Writing – review & editing, Supervision, Resources, Funding acquisition, Conceptualization.

## Declaration of competing interest

There is no conflict of interest.

## Supplementary materials

Supplementary material associated with this article can be found, in the online version, at doi:10.1016/j.electacta.2026.148957.

## Data availability

Data will be made available on request.

## References

[1] L. Geiser, J.-L. Veuthey, Non-aqueous capillary electrophoresis 2005–2008, Electrophoresis 30 (2009) 36–49, https://doi.org/10.1002/elps.200800494.
[2] E. Kenndler, A critical overview of non-aqueous capillary electrophoresis. Part I: mobility and separation selectivity, J. Chromatogr. A 1335 (2014) 16–30, https://doi.org/10.1016/j.chroma.2014.01.010.
[3] A.A. Elbashir, R.E.E. Elgorashe, A.O. Alnajjar, H.Y. Aboul-Enein, Application of capillary electrophoresis with capacitively coupled contactless conductivity detection (CE-C4D): 2017–2020, Crit. Rev. Anal. Chem. 52 (2022) 535–543, https://doi.org/10.1080/10408347.2020.1809340.
[4] P. Kubáň, P.C. Hauser, Ten years of axial capacitively coupled contactless conductivity detection for CZE – a review, Electrophoresis 30 (2009) 176–188, https://doi.org/10.1002/elps.200800478.
[5] A. Beutner, B. Scherer, F.-M. Matysik, Dual detection for non-aqueous capillary electrophoresis combining contactless conductivity detection and mass spectrometry, Talanta 183 (2018) 33–38, https://doi.org/10.1016/j.talanta.2018.02.012.
[6] G.K.E. Scriba, Non-aqueous capillary electrophoresis–mass spectrometry, J. Chromatogr. A 1159 (2007) 28–41, https://doi.org/10.1016/j.chroma.2007.02.005.
[7] K. Yao, R. Jiang, P. Wang, J. Zhang, B. Shao, X. Ding, Comparison of aqueous and non-aqueous capillary electrophoresis for the determination of four benzalkonium chloride homologues in compound chemical disinfectants, Heliyon. 10 (2024) e31797, https://doi.org/10.1016/j.heliyon.2024.e31797.
[8] R. Carabias-Martínez, E. Rodríguez-Gonzalo, E. Miranda-Cruz, J. Domínguez-Álvarez, J. Hernández-Méndez, Comparison of a non-aqueous capillary electrophoresis method with high performance liquid chromatography for the determination of herbicides and metabolites in water samples, J. Chromatogr. A 1122 (2006) 194–201, https://doi.org/10.1016/j.chroma.2006.04.017.
[9] X. Wang, K. Li, L. Yao, C. Wang, A. Van Schepdael, Recent advances in vitamins analysis by capillary electrophoresis, J. Pharm. Biomed. Anal. 147 (2018) 278–287, https://doi.org/10.1016/j.jpba.2017.07.030.
[10] F.-M. Matysik, Application of non-aqueous capillary electrophoresis with electrochemical detection to the determination of nicotine in tobacco, J. Chromatogr. A 853 (1999) 27–34, https://doi.org/10.1016/S0021-9673(99)00512-9.
[11] J.H.T. Luong, A. Hilmi, A.-L. Nguyen, Non-aqueous capillary electrophoresis equipped with amperometric detection for analysis of chlorinated phenolic compounds, J. Chromatogr. A 864 (1999) 323–333, https://doi.org/10.1016/S0021-9673(99)01032-8.
[12] U. Backofen, F.-M. Matysik, C.E. Lunte, Determination of cannabinoids in hair using high-pH non-aqueous electrolytes and electrochemical detection: some aspects of sensitivity and selectivity, J. Chromatogr. A 942 (2002) 259–269, https://doi.org/10.1016/S0021-9673(01)01348-6.
[13] U. Backofen, F.-M. Matysik, W. Hoffmann, C.E. Lunte, Analysis of illicit drugs by non-aqueous capillary electrophoresis and electrochemical detection, Fresenius. J. Anal. Chem. 367 (2000) 359–363, https://doi.org/10.1007/s002160000371.
[14] M. Baroch, H. Dejmková, F.-M. Matysik, Determination of trimetazidine in urine by capillary electrophoresis with amperometric detection, Monatsh. Chem. 154 (2023) 1013–1018, https://doi.org/10.1007/s00706-023-03083-2.
[15] S. Ivakh, M. Koall, J. Barek, F.-M. Matysik, Comparative electrochemical study of oxidative nicarbazin determination in non-aqueous media: differential pulse voltammetry vs. capillary electrophoresis with amperometric detection, Talanta 288 (2025) 127729, https://doi.org/10.1016/j.talanta.2025.127729.
[16] D. Böhm, M. Koall, F.-M. Matysik, Combining amperometry and mass spectrometry as a dual detection approach for capillary electrophoresis, Electrophoresis 44 (2023) 492–500, https://doi.org/10.1002/elps.202200228.
[17] M. Koall, D. Böhm, T. Herl, F.-M. Matysik, Sensitive and selective determination of the neonicotinoid nitenpyram utilizing capillary electrophoresis hyphenated to amperometric detection/mass spectrometry, Electroanalysis. 35 (2023) e202300238, https://doi.org/10.1002/elan.202300238.
[18] H.-H. Rüttinger, A. Radschuweit, Determination of peroxides by capillary zone electrophoresis with amperometric detection, J. Chromatogr. A 868 (2000) 127–134, https://doi.org/10.1016/S0021-9673(99)01162-0.
[19] A. Hilmi, J.H.T. Luong, A.-L. Nguyen, Development of electrokinetic capillary electrophoresis equipped with amperometric detection for analysis of explosive compounds, Anal. Chem. 71 (1999) 873–878, https://doi.org/10.1021/ac980945n.
[20] J. Fischer, J. Barek, Separation and detection of nitrophenols at capillary electrophoresis microchips with amperometric detection, Electroanalysis 18 (2006) 195–199, https://doi.org/10.1002/elan.200503393.
[21] A. Schizodimou, G. Kyriacou, C. Lambrou, Electrochemical reduction of dichlorodifluoromethane in acetonitrile medium to useful fluorinated compounds, J. Electroanal. Chem. 471 (1999) 26–31, https://doi.org/10.1016/S0022-0728(99)00244-2.
[22] L. Benedetti, M. Borsari, D. Dallari, C. Fontanesi, G. Grandi, G. Gavioli, Electrochemical reduction of benzamide and their o- and p-halo-derivatives in non-aqueous solvents, Electrochim. Acta 39 (1994) 2723–2728, https://doi.org/10.1016/0013-4686(94)E0178-3.
[23] G. Damián Chanique, A. Heraldo Arévalo, M. Alicia Zon, H. Fernández, Electrochemical reduction of patulin and 5-hydroxymethylfurfural in both neutral and acid non-aqueous media. Their electroanalytical determination in apple juices, Talanta 111 (2013) 85–92, https://doi.org/10.1016/j.talanta.2013.02.041.
[24] P. Broomandi, M. Guney, J.R. Kim, F. Karaca, Soil contamination in areas impacted by military activities: a critical review, Sustainability 12 (2020), https://doi.org/10.3390/su12219002.
[25] J. Tiwari, P. Tarale, S. Sivanesan, A. Bafana, Environmental persistence, hazard, and mitigation challenges of nitroaromatic compounds, Environ. Sci. Pollut. Res. 26 (2019) 28650–28667, https://doi.org/10.1007/s11356-019-06043-8.
[26] J. Fischer, L. Vanourkova, A. Danhel, V. Vyskocil, K. Cizek, J. Barek, K. Peckova, B. Yosypchuk, T. Navratil, Voltammetric determination of nitrophenols at a silver solid amalgam electrode, Int. J. Electrochem. Sci. 2 (2007) 226–234, https://doi.org/10.1016/S1452-3981(23)17068-4.
[27] B. Dinesh, A. Aadhav, K.S.S. Devi, U.M. Krishnan, Electrocatalytic reduction of 2,4-dinitrophenol on carbon black-modified glassy carbon electrode and its selective recognition in cold beverages, Carbon Lett. 32 (2022) 1017–1029, https://doi.org/10.1007/s42823-022-00334-w.
[28] H. Houcini, F. Laghrib, M. Bakasse, S. Lahrich, M.A. El Mhammedi, Catalytic activity of gold for the electrochemical reduction of p-nitrophenol: analytical application, Int. J. Environ. Anal. Chem. 100 (2020) 1566–1577, https://doi.org/10.1080/03067319.2019.1655558.
[29] M. Mahyari, Electrochemical determination of picric acid based on platinum nanoparticles–reduced graphene oxide composite, Int. J. Environ. Anal. Chem. 96 (2016) 1455–1468, https://doi.org/10.1080/03067319.2016.1268606.
[30] P. Palatzky, F.-M. Matysik, Development and characterization of a novel semiautomated arrangement for electrochemically assisted injection in combination with capillary electrophoresis time-of-flight mass spectrometry, Electrophoresis 33 (2012) 2689–2694, https://doi.org/10.1002/elps.201200088.
[31] P. Palatzky, A. Zöpfl, T. Hirsch, F.-M. Matysik, Electrochemically assisted injection in combination with capillary electrophoresis-mass spectrometry (EAI-CE-MS) – Mechanistic and quantitative studies of the reduction of 4-nitrotoluene at various carbon-based screen-printed electrodes, Electroanalysis 25 (2013) 117–122, https://doi.org/10.1002/elan.201200393.
[32] X. Guo, Z. Wang, S. Zhou, The separation and determination of nitrophenol isomers by high-performance capillary zone electrophoresis, Talanta 64 (2004) 135–139, https://doi.org/10.1016/j.talanta.2004.01.020.
[33] J.L. Miller, D. Shea, M.G. Khaledi, Separation of acidic solutes by non-aqueous capillary electrophoresis in acetonitrile-based media: combined effects of deprotonation and heteroconjugation, J. Chromatogr. A 888 (2000) 251–266, https://doi.org/10.1016/S0021-9673(00)00467-2.
[34] R. Schmid, S. Heuckeroth, A. Korf, A. Smirnov, O. Myers, T.S. Dyrlund, R. Bushuiev, K.J. Murray, N. Hoffmann, M. Lu, A. Sarvepalli, Z. Zhang, M. Fleischauer, K. Dührkop, M. Wesner, S.J. Hoogstra, E. Rudt, O. Mokshyna, C. Brungs, K. Ponomarov, L. Mutabdžija, T. Damiani, C.J. Pudney, M. Earll, P. O. Helmer, T.R. Fallon, T. Schulze, A. Rivas-Ubach, A. Bilbao, H. Richter, L.-F. Nothias, M. Wang, P.O. Orešič, J.-K. Weng, S. Böcker, A. Jeibmann, H. Hayen, U. Karst, P.C. Dorrestein, D. Petras, X. Du, T. Pluskal, Integrative analysis of multimodal mass spectrometry data in MZmine 3, Nat. Biotechnol. 41 (2023) 447–449, https://doi.org/10.1038/s41587-023-01690-2.
[35] N. Ramaswamy, S. Mukerjee, Fundamental mechanistic understanding of electrocatalysis of oxygen reduction on Pt and non-Pt surfaces: acid versus alkaline media, Adv. Phys. Chem. 2012 (2012) 491604, https://doi.org/10.1155/2012/491604.
[36] C.C.M. Neumann, E. Laborda, K. Tschulik, K.R. Ward, R.G. Compton, Performance of silver nanoparticles in the catalysis of the oxygen reduction reaction in neutral media: efficiency limitation due to hydrogen peroxide escape, Nano Res. 6 (2013) 511–524, https://doi.org/10.1007/s12274-013-0328-4.

[37] J. Kim, A.A. Gewirth, Mechanism of oxygen electroreduction on gold surfaces in basic media, J. Phys. Chem. B 110 (2006) 2565–2571, https://doi.org/10.1021/jp0549529.
[38] A. Lasia, Hydrogen evolution reaction, in: Handbook of Fuel Cells: Fundamentals, Technology and Applications, 2, Wiley, Chichester, 2003, pp. 414–440, https://doi.org/10.1002/9780470974001.f204033.
[39] Q. Li, C. Batchelor-McAuley, N.S. Lawrence, R.S. Hartshorne, R.G. Compton, Anomalous solubility of oxygen in acetonitrile/water mixture containing tetra-n-butylammonium perchlorate supporting electrolyte; the solubility and diffusion coefficient of oxygen in anhydrous acetonitrile and aqueous mixtures, J. Electroanal. Chem. 688 (2013) 328–335, https://doi.org/10.1016/j.jelechem.2012.07.039.